Scientia Iranica A (2017) 24(6), 2776–2792

Sharif University of Technology
Scientia Iranica
Transactions A: Civil Engineering
www.scientiairanica.com

Generalized implicit multi-time-step integration for nonlinear dynamic analysis

J. Alamatian*

Department of Civil Engineering, Mashhad Branch, Islamic Azad University, Mashhad, P.O. Box: 91735-413, Iran.

Received 22 December 2015; received in revised form 11 June 2016; accepted 25 February 2017

KEYWORDS
Multi time step;
Numerical integration;
Implicit method;
Dynamic analysis;
Conditional stability;
Higher accuracy.

Abstract. This paper deals with a generalized multi-time-step integration used for structural dynamic analysis. The proposed method presents three kinds of implicit schemes in which the accelerations and velocities of the previous steps are utilized to integrate the equations of motion. This procedure employs three groups of weighted factors calculated by minimizing the numerical errors of displacement and velocity in Taylor series expansion. Moreover, a comprehensive study on mathematical stability of the proposed technique, which is performed based on the amplification matrices, proves that the new method is more stable than existing schemes such as IHOA. For numerical verification, a wide range of dynamic systems, including linear and nonlinear, single and multi degrees of freedom, damped and undamped, as well as forced and free vibrations from finite-element and finite-difference methods, are analyzed. These numerical studies demonstrate that efficiency and accuracy of the proposed method are higher than those of other techniques.

1. Introduction

Numerical time integrations are widely used for structural dynamic analysis, especially in nonlinear cases, due to difficulties in formulating the closed-form solution to differential equations of motion, which could be written in the following form:

$$\mathbf{M}\ddot{\mathbf{D}} + \mathbf{C}\dot{\mathbf{D}} + \mathbf{f} = \mathbf{P}, \tag{1}$$

$$\mathbf{D}_{(t=0)} = \mathbf{D}_0, \quad \dot{\mathbf{D}}_{(t=0)} = \dot{\mathbf{D}}_0. \tag{2}$$

Here, $\mathbf{M}$, $\mathbf{C}$, $\mathbf{f}$, and $\mathbf{P}$ are mass matrix, damping matrix, internal and external forces vectors, respectively. Also, $\mathbf{D}$ is the nodal displacement vector while superimposed dots denote differential with respect to time. Moreover, $\mathbf{D}_0$ and $\dot{\mathbf{D}}_0$ are initial conditions for displacement and velocity vectors at $t = 0$, respectively. Numerical methods calculate the structural responses, i.e. displacement, velocity, and acceleration vectors, in small time increments, called time steps. In other words, systematic time integrations are performed for each increment until the time duration, which is divided into finite increments, is completed. These methods may have three main concerns, i.e. stability, accuracy, and simplicity. Based on such criteria, numerical integrations could be classified into three groups: implicit, explicit, and predictor-corrector procedures. Accuracy and stability of implicit integrations are higher than both explicit and predictor-corrector schemes. In each time step of these methods, dynamic equation of motion (Eq. (1)) is converted to a static system by deriving equivalent stiffness matrix and equivalent external force vector of structure, i.e.:

$$\mathbf{S}_{EQ}\mathbf{D} = \mathbf{P}_{EQ}, \tag{3}$$

*. *E-mail address: alamatian@mshdiau.ac.ir*

doi: 10.24200/sci.2017.4167

where $\mathbf{S}_{EQ}$ and $\mathbf{P}_{EQ}$ are equivalent stiffness matrix and equivalent load vector of dynamic analysis, respectively. Running a statically analysis in each time step would be a difficult and time-consuming procedure. Newmark-β method, Wilson-θ scheme, HHT-α procedure [1], WBZ-α integration [2], generalized-α method [3], Newmark multi-time-step approach [4], third-order time step integration [5], the Newmark complex time step [6], the time weighted function procedure [7], the generalized single step integration [8], the NØrsett time integration [9], the composite time integration [10], the higher order acceleration function [11], the implicit integration based on conserving energy and momentum [12], the Green function approach [13,14], the precise integration methods [15], the IHOA [16], and the implicit integration combined with the finite-element method [17] are some of the implicit integrations.

On the other hand, explicit procedures, run completely by vector operations, are the most simple time integrations. However, it is necessary to choose very small time steps for guaranteeing stability and improving accuracy of explicit methods. Some of the explicit integrations are the generalized weighted residual approach [18], *SSpj* method [19], β_m algorithm [20], Hoff-Taylor approach [21], etc.

The predictor-corrector methods try to assemble accuracy and stability of implicit integrations with the simplicity of explicit techniques, simultaneously. In these procedures, prediction and correction stages are performed by explicit and implicit integrations, respectively. Such a procedure improves stability of explicit integrations and leads to a more simple integration in comparison with implicit techniques. Zhai's scheme [22] includes the modified PC technique [23] and the $PC-m$ integration [24] which are some examples of the predictor-corrector methods.

It should be noted that by changing weighted factors, many of the previous implicit integrations have the ability to use as an explicit or predictor-corrector scheme [16,25,26]. For example, the implicit higher-order accuracy integration method (called IHOA) presents the $PC-m$ integration [24]. Therefore, stability and accuracy of each predictor-corrector integration directly depend on the specifications of implicit method used. As a result, proposing an implicit method with higher stability and accuracy is a necessary condition for formulating an improved predictor-corrector method. For this purpose, the generalized implicit higher-order time integration is proposed here. Accuracy and stability analyses are performed based on Taylor series expansion and amplification matrices, respectively. Finally, some linear and nonlinear numerical dynamic analyses are performed to verify the ability of the proposed integration.

2. The Generalized Implicit Higher Order Accuracy (G-IHOA) integration

Numerical time integrations, called step-by-step methods, are utilized for solving Eq. (1), which is a time differential equation. From a mathematical point of view, the main concern may be creating continuity between displacement's higher-order time derivatives (third order, fourth order, etc.). The reason for this subject is that the first and second orders of displacement's time derivatives only exist in dynamic equilibrium equation (Eq. (1)). In other words, there is no relationship for controlling and checking higher-order time derivatives continuity. This subject has a considerable effect on stability and accuracy of numerical integrations so that researchers can try to improve this defect in two manners: utilizing higher-order time derivatives of a single previous increment [27] and proposing multi-time step schemes [28]. The first approach could be used in single step time integrations; however, it has some difficulties, especially in the beginning of the process when higher-order derivatives should be estimated [19,20]. The multi-time-step integrations, which use information of several previous time increments to integrate the current step, are another way for satisfying the continuity of higher-order time derivatives [16,22,24,28]. In spite of more requirement memory, multi-time-step integrations are more accurate and efficient than single-step methods. Here, a new multi-time-step integration, called Generalized Implicit Higher Order Accuracy, i.e. G-IHOA method, is presented based on the idea of multi-time-step integrations. The fundamental relationships of G-IHOA are proposed as follows:

$$\begin{aligned}\mathbf{D}^{n+1} =&\mathbf{D}^n + \Delta t\left(1-\alpha'-\sum_{i=1}^{m-1}\alpha_i\right)\dot{\mathbf{D}}^n \\ &+\Delta t\alpha'\dot{\mathbf{D}}^{n+1}+\Delta t\sum_{i=1}^{m-1}\alpha_i\dot{\mathbf{D}}^{n-i} \\ &+\Delta t^2\left(\frac{1}{2}-\beta'\sum_{i=1}^{m-1}\beta_i\right)\ddot{\mathbf{D}}^n+\Delta t^2\beta'\ddot{\mathbf{D}}^{n+1} \\ &+\Delta t^2\sum_{i=1}^{m-1}\beta_i\ddot{\mathbf{D}}^{n-i},\end{aligned} \tag{4}$$

$$\begin{aligned}\dot{\mathbf{D}}^{n+1} =&\dot{\mathbf{D}}^n+\Delta t\left(1-\gamma'-\sum_{i=1}^{m-1}y_i\right)\ddot{\mathbf{D}}^n \\ &+\Delta t\gamma'\ddot{\mathbf{D}}^{n+1}+\Delta t\sum_{i=1}^{m-1}\gamma_i\ddot{\mathbf{D}}^{n-i},\end{aligned} \tag{5}$$

where α', β', γ', and $\alpha_i,\beta_i,\gamma_i$, $i=1,2,...,m-1$, are weighted factors which control the stability and accuracy of the proposed G-IHOA method. Here, m is an integration's order and superscript n means values at the nth time step (time t^n). Also, Δt is time step of numerical dynamic analysis. In this method, displacement of the current time step is proposed as a function of velocities and accelerations of several previous increments (Eq. (4)). Moreover, accelerations of the previous steps are used to formulate the current velocity (Eq. (5)). In a special case, if $\alpha' = \alpha_1 = \alpha_2 = ... = \alpha_{m-1} = 0$, the above relationships present IHOA integration [16]. Another interesting version of G-IHOA is obtained when $\beta' = \beta_1 = \beta_2 = ... = \beta_{m-1} = 0$. This version of G-IHOA is called N-IHOA [29]. In N-IHOA method, displacement and velocity of the current time step are assumed functions of the velocities and accelerations of several previous time steps, respectively [29]. As a result, Eqs. (4) and (5) could present three kinds of implicit time integration methods, i.e. IHOA, N-IHOA, and G-IHOA. It should be noted that current paper deals with specifications of G-IHOA, proposed here. All formulations are performed based on the generalized integration (G-IHOA), i.e. Eqs. (4) and (5). Then, results could be summarized for IHOA and N-IHOA by removing the corresponding sentences.

Assume that the integration procedure is at $n+1$st step (the current increment). By substituting Eq. (5) into Eq. (4), acceleration of the current step is obtained:

$$\begin{aligned}\ddot{\mathbf{D}}^{n+1} =& \frac{1}{\Delta t^2(\alpha'\gamma'+\beta')}\Bigg(\mathbf{D}^{n+1}-\mathbf{D}^n \\ &- \Delta t(1-\sum_{i=1}^{m-1}\alpha_i)\dot{\mathbf{D}}^n - \Delta t^2\bigg(\frac{1}{2}-\beta' \\ &- \sum_{i=1}^{m-1}\beta_i+\alpha'-\alpha'\gamma'-\alpha'\sum_{i=1}^{m-1}\gamma_i\bigg)\ddot{\mathbf{D}}^n \\ &- \Delta t^2\sum_{i=1}^{m-1}(\alpha'\gamma_i+\beta_i)\ddot{\mathbf{D}}^{n-i}\Bigg). \qquad (6)\end{aligned}$$

Utilizing Eq. (6) in Eq. (5) gives:

$$\begin{aligned}\dot{\mathbf{D}}^{n+1} =& \dot{\mathbf{D}}^n + \Delta t\bigg(1-\gamma'-\sum_{i=1}^{m-1}\gamma_i\bigg)\ddot{\mathbf{D}}^n \\ &+ \frac{\gamma'}{\Delta t(\alpha'\gamma'+\beta')}\Bigg(\mathbf{D}^{n+1}-\mathbf{D}^n \\ &- \Delta t(1-\sum_{i=1}^{m-1}\alpha_i)\dot{\mathbf{D}}^n - \Delta t^2\bigg(\frac{1}{2}-\beta' \\ &- \sum_{i=1}^{m-1}\beta_i+\alpha'-\alpha'\gamma'-\alpha'\sum_{i=1}^{m-1}\gamma_i\bigg)\ddot{\mathbf{D}}^n \\ &- \Delta t^2\sum_{i=1}^{m-1}(\alpha'\gamma_i+\beta_i)\ddot{\mathbf{D}}^{n-i}\Bigg) \\ &+ \Delta t\sum_{i=1}^{m-1}\gamma_i\ddot{\mathbf{D}}^{n-i}. \qquad (7)\end{aligned}$$

If Eqs. (6) and (7) are substituted into the dynamic equilibrium equation (Eq. (1) with superscript $n+1$), the equivalent stiffness matrix and the equivalent load vector of the proposed G-IHOA integration are formulated as follows:

$$\begin{aligned}\mathbf{S}_{EQ}^{n+1} =& \frac{1}{\Delta t^2(\alpha'\gamma'+\beta')}\mathbf{M}^{n+1} + \frac{\gamma'}{\Delta t(\alpha'\gamma'+\beta')}\mathbf{C}^{n+1} \\ &+ \mathbf{S}^{n+1}, \qquad (8a)\end{aligned}$$

$$\begin{aligned}\mathbf{P}_{EQ}^{n+1} =& \mathbf{P}(t^{n+1}) + \mathbf{M}^{n+1}\Bigg(\mathbf{D}^n + \Delta t(1-\sum_{i=1}^{m-1}\alpha_i)\dot{\mathbf{D}}^n \\ &+ \Delta t^2\bigg(\frac{1}{2}-\beta'-\sum_{i=1}^{m-1}\beta_i+\alpha-\alpha'\gamma' \\ &- \alpha'\sum_{i=1}^{m-1}\gamma_i\bigg)\ddot{\mathbf{D}}^n + \Delta t^2\sum_{i=1}^{m-1}(\alpha'\gamma_i+\beta_i)\ddot{\mathbf{D}}^{n-i}\Bigg) \\ &- \mathbf{C}^{n+1}\Bigg(\dot{\mathbf{D}}^n + \Delta t(1-\gamma'-\sum_{i=1}^{m-1}\gamma_i)\ddot{\mathbf{D}}^n \\ &- \frac{\gamma'}{\Delta t(\alpha'\gamma'+\beta')}\bigg(\mathbf{D}^n + \Delta t(1-\sum_{i=1}^{m-1}\alpha_i)\dot{\mathbf{D}}^n \\ &+ \Delta t^2\bigg(\frac{1}{2}-\beta'-\sum_{i=1}^{m-1}\beta_i+\alpha'-\alpha'\gamma' \\ &- \alpha'\sum_{i=1}^{m-1}\gamma_i\bigg)\ddot{\mathbf{D}}^n + \Delta t^2\sum_{i=1}^{m-1}(\alpha'\gamma_i+\beta_i)\ddot{\mathbf{D}}^{n-i}\bigg) \\ &+ \Delta t\sum_{i=1}^{m-1}\gamma_i\ddot{\mathbf{D}}^{n-i}\Bigg). \qquad (8b)\end{aligned}$$

By substituting both the equivalent stiffness matrix and the equivalent force vector (Eqs. (8a) and (8b)) into Eq. (3) and solving a system of simultaneous equations, displacement vector of the current time step (time t^{n+1}) is obtained. Then, acceleration and velocity vectors of the $n+1$th time step (current time step) could be calculated from Eqs. (6) and (7), respectively. This procedure is iterated for next time steps until required analysis time is completed.

If $m > 1$, the required data of the previous increments is not available at the first time step ($n = 1$). To overcome this difficulty, the first increment could be started by $m = 1$. At the end of this stage, two equilibrium points (n and $n-1$) will be available so that the second time step of G-IHOA integration is performed by $m = 2$. At this time, three dynamic equilibrium points of the previous steps (n, $n-1$, and $n-2$) exist and the next increment could be started by $m = 3$. Briefly, the integration's order increases one unit by running each step from the starting increment until it reaches the selected rank. In this technique, the personal judgment does not have any effect on the integration and the procedure could be performed automatically.

It should be noted that the equivalent stiffness matrix and the equivalent force vector of N-IHOA can be obtained by removing the corresponding sentences' occurrences of parameters $\beta', \beta_1, \beta_2, ...\beta_{m-1}$ from Eqs. (8a) and (8b), respectively [29]:

$$\mathbf{S}_{EQ}^{n+1} = \frac{1}{\alpha'\gamma'\Delta t^2}\mathbf{M}^{n+1} + \frac{1}{\alpha'\Delta t}\mathbf{C}^{n+1} + \mathbf{S}^{n+1}, \tag{9a}$$

$$\begin{aligned}\mathbf{P}_{EQ}^{n+1} =& \mathbf{P}_{(t^{n+1})} + \frac{1}{\Delta t^2\alpha'\gamma'}\mathbf{M}^{n+1}\Bigg(\mathbf{D}^n \\ &+ \Delta t(1 - \sum_{i=1}^{m-1}\alpha_i)\dot{\mathbf{D}}^n + \Delta t\sum_{i=1}^{m-1}\alpha_i\dot{\mathbf{D}}^{n-i}\Bigg) \\ &+ \frac{1}{\gamma'}\mathbf{M}^{n+1}\Bigg(\Bigg(1-\gamma'-\sum_{i=1}^{m-1}\gamma_i\Bigg)\ddot{\mathbf{D}}^n \\ &+ \sum_{i=1}^{m-1}\gamma_i\ddot{\mathbf{D}}^{n-i}\Bigg) + \frac{1}{\Delta t\alpha'}\mathbf{C}^{n+1}\Bigg(\mathbf{D}^n \\ &+ \Delta t(1-\alpha'-\sum_{i=1}^{m-1}\alpha_i)\dot{\mathbf{D}}^n \\ &+ \Delta t\sum_{i=1}^{m-1}\alpha_i\dot{\mathbf{D}}^{n-i}\Bigg).\end{aligned} \tag{9b}$$

Similar formulation has been performed for IHOA method [16].

3. Accuracy analysis

Each numerical time integration deals with two concerns: stability and accuracy. In this way, the most common strategy suggests that the integration's parameters are calculated for the highest possible accuracy, and stability condition is controlled by limiting time step size of dynamic analysis. On this base, the weighted factors of G-IHOA are calculated for maximum numerical accuracy. For accuracy order m, there are $3 \times m$ free parameters in displacement and velocity relationships (Eqs. (4) and (5)). First, error functions of displacement and velocity could be defined as follows:

$$\mathbf{R}_D^{n+1} = \mathbf{D}^{n+1} - \mathbf{D}_{\text{Exact}}^{n+1}, \tag{10}$$

$$\mathbf{R}_V^{n+1} = \dot{\mathbf{D}}^{n+1} - \dot{\mathbf{D}}_{\text{Exact}}^{n+1}, \tag{11}$$

where $\mathbf{R}_D^{n+1}$ and $\mathbf{R}_V^{n+1}$ are displacement and velocity residuals (errors) at time t^{n+1}, respectively. Based on Taylor series expansion, the exact solutions of displacement ($\mathbf{D}_{\text{Exact}}^{n+1}$) and velocity ($\dot{\mathbf{D}}_{\text{Exact}}^{n+1}$) are also achieved:

$$\begin{aligned}\mathbf{D}_{\text{Exact}}^{n+1} =& \sum_{k=0}^{\infty}\frac{\Delta t^k}{k!}\mathbf{D}^{k^n} = \mathbf{D}^n + \Delta t\dot{\mathbf{D}}^n + \frac{\Delta t^2}{2}\ddot{\mathbf{D}}^n \\ &+ \frac{\Delta t^3}{6}\mathbf{D}^{3^n} + \frac{\Delta t^4}{24}\mathbf{D}^{4^n} + ...,\end{aligned} \tag{12}$$

$$\begin{aligned}\dot{\mathbf{D}}_{\text{Exact}}^{n+1} =& \sum_{k=0}^{\infty}\frac{\Delta t^k}{k!}\mathbf{D}^{k+1^n} = \dot{\mathbf{D}}^n + \Delta t\ddot{\mathbf{D}}^n \\ &+ \frac{\Delta t^2}{2}\mathbf{D}^{3^n} + \frac{\Delta t^3}{6}\mathbf{D}^{4^n} + \frac{\Delta t^4}{24}\mathbf{D}^{5^n} + ...\end{aligned} \tag{13}$$

Here, $\mathbf{D}^{k^n}$ shows the kth displacement's derivative at the nth time increment. For using Eqs. (4) and (5) in Eqs. (10) and (11), it is necessary to formulate velocities and accelerations of several previous time steps ($n-1$, $n-2$, etc.) as functions of the higher-order derivatives of displacement at the nth increment. For this propose, the inverse expansions of velocities and accelerations give [16]:

$$\dot{\mathbf{D}}^{n-i} = \sum_{k=0}^{\infty}\frac{(-1)^k\Delta t^k}{k!}\mathbf{D}^{k+1^{n-i+1}} \quad i = 1,2,...,m, \tag{14}$$

$$\ddot{\mathbf{D}}^{n-i} = \sum_{k=0}^{\infty}\frac{(-1)^k\Delta t^k}{k!}\mathbf{D}^{k+2^{n-i+1}} \quad i = 1,2,...,m. \tag{15}$$

A similar relationship could be written for the jth order of displacement's derivative of some previous time steps ($n-i$th):

$$\mathbf{D}^{j^{n-i}} = \sum_{k=0}^{\infty}\frac{(-1)^k\Delta t^k}{k!}\mathbf{D}^{j-k^{n-i+1}}, \quad i = 1,2,...m \quad j = 1,2,...,\infty. \tag{16}$$

If Eqs. (14) to (16) are iterated successively, the previous time steps' velocities and accelerations are formulated in terms of displacement[s derivatives at time t^n. For example, displacement and velocity functions for the first, second, and third accuracy orders of the G-IHOA (m = 1, 2 and 3) are obtained as follows:

$$\begin{aligned}\mathbf{D}^{n+1} =& \mathbf{D}^n + \Delta t\dot{\mathbf{D}}^n + \left(\frac{1}{2}+\alpha'\right)\Delta t^2\ddot{\mathbf{D}}^n \\ &+ \left(\frac{\alpha'}{2}+\beta'\right)\Delta t^3\mathbf{D}^{3^n}\{D^3\}^n \\ &+ \left(\frac{\alpha'}{6}+\frac{\beta'}{2}\right)\Delta t^4\mathbf{D}^{4^n}+... \qquad m=1,\end{aligned} \tag{17}$$

$$\dot{\mathbf{D}}^{n+1} = \dot{\mathbf{D}}^n + \Delta t\ddot{\mathbf{D}}^n + \gamma'\Delta t^2\mathbf{D}^{3^n} + \frac{\gamma'\Delta t^3}{2}\mathbf{D}^{4^n} + ... \qquad m=1, \tag{18}$$

$$\begin{aligned}\mathbf{D}^{n+1} =& \mathbf{D}^N + \Delta t\dot{\mathbf{D}}^n + \left(\frac{1}{2}+\alpha'-\alpha_1\right)\Delta t^2\ddot{\mathbf{D}}^n \\ &+ \left(\frac{\alpha'}{2}+\frac{\alpha_1}{2}+\beta'-\beta_1\right)\Delta t^3\mathbf{D}^{3^n} \\ &+ \left(\frac{\alpha'}{6}-\frac{\alpha_1}{6}+\frac{\beta'}{2}+\frac{\beta_1}{2}\right)\Delta t^4\mathbf{D}^{4^n} \\ &+ ... \qquad m=2,\end{aligned} \tag{19}$$

$$\begin{aligned}\dot{\mathbf{D}}^{n+1} =& \dot{\mathbf{D}}^n + \Delta t\ddot{\mathbf{D}}^n + (\gamma'-\gamma_1)\Delta t^2\mathbf{D}^{3^n} \\ &+ \left(\frac{\gamma'}{2}+\frac{\gamma_1}{2}\right)\Delta t^3\mathbf{D}^{4^n}+... \qquad m=2,\end{aligned} \tag{20}$$

$$\begin{aligned}\mathbf{D}^{n+1} =& \mathbf{D}^n + \Delta t\dot{\mathbf{D}}^n + \left(\frac{1}{2}+\alpha'-\alpha_1-2\alpha_2\right)\Delta t^2\ddot{\mathbf{D}}^n \\ &+ \left(\frac{\alpha'}{2}+\frac{\alpha_1}{2}+2\alpha_2+\beta'-\beta_1\right. \\ &\left.-2\beta_2\right)\Delta t^3\mathbf{D}^{3^n} + \left(\frac{\alpha'}{6}-\frac{\alpha_1}{6}-\frac{4\alpha_2}{3}+\frac{\beta'}{2}\right. \\ &\left.+\frac{\beta_1}{2}+2\beta_2\right)\Delta t^4\mathbf{D}^{4^n}+... \qquad m=3,\end{aligned} \tag{21}$$

$$\begin{aligned}\dot{\mathbf{D}}^{n+1} =& \dot{\mathbf{D}}^n + \Delta t\ddot{\mathbf{D}}^n + (\gamma'-\gamma_1-2\gamma_2)\Delta t^2\mathbf{D}^{3^n} \\ &+ \left(\frac{\gamma'}{2}+\frac{\gamma_1}{2}+2\gamma_2\right)\Delta t^3\mathbf{D}^{4^n} + \left(\frac{\gamma'}{6}\right. \\ &\left.-\frac{\gamma_1}{6}-\frac{4\gamma_2}{3}\right)\Delta t^4\mathbf{D}^{5^n}+... \qquad m=3.\end{aligned} \tag{22}$$

From the mathematical point of view, the weighted factors should be determined so that a good number of derivatives/coefficients are equalized to their corresponding values in Taylor series expansion (Eqs. (12) and (13)). It is clear that lower derivatives come before higher ones. By running this approach for displacement and velocity sentences, two linear systems of equations are obtained for each accuracy order such as m:

$$(\mathbf{Z}_D)_{2m\times 2m}\begin{Bmatrix}\alpha'\\ \alpha_1\\ \vdots\\ \alpha_{m-1}\\ \beta'\\ \beta_1\\ \vdots\\ \beta_{m-1}\end{Bmatrix}_{2m\times 1} = \begin{Bmatrix}0\\ \frac{1}{3!}\\ \frac{1}{4!}\\ \vdots\\ \frac{1}{(2m+1)!}\end{Bmatrix}_{2m\times 1}, \tag{23}$$

$$(\mathbf{Z}_V)_{m\times m}\begin{Bmatrix}\gamma'\\ \gamma_1\\ \vdots\\ \gamma_{m-1}\end{Bmatrix}_{m\times 1} = \begin{Bmatrix}\frac{1}{2!}\\ \frac{1}{3!}\\ \vdots\\ \frac{1}{(m+1)!}\end{Bmatrix}_{m\times 1}. \tag{24}$$

In these equations, $(\mathbf{Z}_D)_{2m\times 2m}$ and $(\mathbf{Z}_V)_{m\times m}$ are constant matrices, constructed based on derivatives coefficients of displacement and velocity relationships in G-IHOA (e.g. Eqs. (17)-(22)). These matrices are presented for the integration's orders 1, 2, and 3 in the Appendix. By solving linear systems of Eqs. (23) and (24), the optimum weighted factors of the proposed G-IHOA integration are obtained. These linear systems have been solved for accuracy orders between 0 and 6, and the optimum values of weighted factors α, β, and γ are inserted in Tables 1, 2 and 3, respectively.

On the other hand, N-IHOA, which is a special case of G-IHOA, could be obtained if $\beta' = \beta_1 = \beta_2 = ... = \beta_{m-1} = 0$ [29]. Here, Eq. (24) does not vary because it does not depend on parameters β. However, Eq. (23) reduces to the following system [29]:

$$\mathbf{Z}_{m\times m}\begin{Bmatrix}\alpha'\\ \alpha_1\\ \vdots\\ \alpha_{m-1}\end{Bmatrix} = \begin{Bmatrix}\frac{1}{2!}\\ \frac{1}{3!}\\ \vdots\\ \frac{1}{(m+1)!}\end{Bmatrix}. \tag{25}$$

It should be noted that right sides of Eqs. (24) and (25) are the same. Moreover, $\mathbf{Z}_{m\times m}$ is an $m\times m$ matrix which is obtained by removing the corresponding elements of parameters $\beta', \beta_1, \beta_2, ..., \beta_{m-1}$ from $(\mathbf{Z}_D)_{2m\times 2m}$. Applying this procedure to the given sample matrices in the Appendix proves that:

$$\mathbf{Z}_{m\times m} = (\mathbf{Z}_V)_{m\times m}. \tag{26}$$

Therefore, Eqs. (24) and (25) are the same. As a result, for N-IHOA integration, $\alpha' = \gamma'$ and $\alpha_i = \gamma_i$ $i =$

Table 1. The optimum weighted factors of parameter α in G-IHOA integration.

m	α'	α_1	α_2	α_3	α_4	α_5
1	0.000000000					
2	0.233333333	0.233333333				
3	0.342559524	0.224107143	0.059226190			
4	0.361454659	0.163492063	0.090281452	0.005799897		
5	0.351354703	0.228075564	0.135189027	−0.03968894	−0.00700802	
6	0.33598339	0.236380165	0.482802794	−0.11317112	−0.12107196	−0.00844023

Table 2. The optimum weighted factors of parameter β in G-IHOA integration.

m	β'	β_1	β_2	β_3	β_4	β_5
1	0.166666667					
2	0.008333333	0.075000000				
3	−0.032242060	0.171726190	0.015575397			
4	−0.037792110	0.184821429	0.038150353	0.001184965		
5	−0.035317520	0.222507566	−0.006281820	−0.026658010	−0.001631330	
6	−0.031878690	0.422198960	−0.039551020	−0.218032110	−0.052557590	−0.001775370

Table 3. The optimum weighted factors of parameter γ in G-IHOA and N-IHOA integrations.

m	γ	γ_1	γ_2	γ_3	γ_4	γ_5
1	0.500000000					
2	0.416666667	−0.083333333				
3	0.375000000	−0.208333333	0.041666667			
4	0.348611111	−0.366666667	0.147222222	−0.026388889		
5	0.329861111	−0.554166667	0.334722222	−0.120138889	0.018750000	
6	0.315591931	−0.768204365	0.62010582	−0.334176587	0.104365079	−0.014269180

$1, 2, ..., m-1$, i.e. there is only one set of independent weighted factors in N-IHOA integration [29]. The weighted factors of N-IHOA method are inserted in Table 3 [29].

The above discussion shows that if accuracy order must be m, numbers of independent weighted factors in the proposed G-IHOA, N-IHOA [29], and IHOA [16] are $3 \times m$, m and $2 \times m$, respectively. Here, N-IHOA integration has the least number of weighted factors, which should be calculated and saved. These subject cases' effects produce that N-IHOA method needs less programming, memory and computational efforts compared with G-IHOA and IHOA schemes.

On the other hand, to compare the proposed G-IHOA scheme with other multi-time-step integrations, such as N-IHOA and IHOA, mathematical accuracy order is defined as the first non-zero derivative's order in residuals of displacement and velocity, i.e. $\mathbf{R}_D^{n+1}$, and $\mathbf{R}_V^{n+1}$. For integration's order m, the mathematical accuracy order of displacement in G-IHOA, N-IHOA, and IHOA will be Δt^{2m+2}, Δt^{m+2}, and Δt^{m+3}, respectively. On the other hand, all three integrations present the velocity with the same accuracy order, i.e. Δt^{m+2}. It is clear that displacement's accuracy of G-IHOA is higher than both N-IHOA and IHOA methods if $m > 1$. As a result, the proposed G-IHOA is more accurate than N-IHOA and IHOA. When $m = 1$, G-IHOA, N-IHOA, and IHOA have the same accuracy.

It should be noted that optimum weighted factors of G-IHOA are unique for each accuracy order, and they are not dependent on the problem specification.

4. Stability conditions

The stability of IHOA method has been previously studied based on the Routh-Hurwitz criterion [16]. This approach has a significant limitation, i.e. it is not able to verify the effect of structural damping on stability. In other words, stability of IHOA has been only obtained for undamped vibrations [16]. For solving this defect, method of amplification matrices is utilized for studying the stability conditions of G-IHOA, N-IHOA, and IHOA integrations [29]. It should be noted that the most common approach to verifying stability of step-by-step time integrations is performed by constructing the amplification matrix [30-32], defined for *free vibration of a single degree of freedom system*:

$$\begin{Bmatrix} d \\ \Delta t\dot{d} \end{Bmatrix}^{n+1} = \mathbf{A}_{2\times 2} \begin{Bmatrix} d \\ \Delta t\dot{d} \end{Bmatrix}^{n}. \qquad (27)$$

Here, $\mathbf{A}_{2\times 2}$ is amplification matrix. The numerical integration will be stable if the highest spectral radius of the amplification matrix is less than 1:

$$|\rho_{\max}| < 1, \tag{28}$$

where $\rho_{\max}$ is the highest eigenvalue of $\mathbf{A}$. For multi-time-step integrations such as G-IHOA, N-IHOA, and IHOA methods, Eq. (27) could be written as follows [29]:

$$\begin{Bmatrix} d \\ \Delta t\dot{d} \end{Bmatrix}^{n+1} = \mathbf{A}^0 \begin{Bmatrix} d \\ \Delta t\dot{d} \end{Bmatrix}^{n} + \mathbf{A}^1 \begin{Bmatrix} d \\ \Delta t\dot{d} \end{Bmatrix}^{n-1} + \mathbf{A}^2 \begin{Bmatrix} d \\ \Delta t\dot{d} \end{Bmatrix}^{n-2} + ... + \mathbf{A}^{m-1} \begin{Bmatrix} d \\ \Delta t\dot{d} \end{Bmatrix}^{n-(m-1)}. \tag{29}$$

Because of using m previous time step to integrate the current increment, there are m amplification matrices in G-IHOA, i.e. $\mathbf{A}^j$ $j = 0, 1, 2, ..., m-1$. In other words, each previous step $(n, n-1...n-j)$ has a specific amplification matrix. Therefore, G-IHOA is stable if all eigenvalues of these amplification matrices satisfy condition (28), i.e.:

$$|\rho^j_{\max}| < 1 \qquad j = 0, 1, 2, ..., m-1, \tag{30}$$

where $\rho^j_{\max}$ is the highest eigenvalue of $\mathbf{A}^j$. To produce amplification matrices of G-IHOA, accelerations should be removed from Eqs. (4) and (5), and they are replaced by displacements and velocities using the dynamic equilibrium equation of free vibration of a single degree of freedom system [29]:

$$\ddot{d}^{n+1} = -\omega^2 d^{n+1} - 2\zeta\zeta\dot{d}^{n+1}, \tag{31}$$

where ζ is viscous damping ratio of structure [33]. By substituting Eq. (31) into Eqs. (4) and (5), the amplification matrices of G-IHOA are obtained as follows:

$$\begin{aligned}\mathbf{A}^0_{2\times2} =& h_1\Bigg[(1+2\gamma'\zeta\Omega)\Bigg(1-\Bigg(\frac{1}{2}-\beta' - \sum_{i=0}^{m-1}\beta_i\Bigg)\Omega^2\Bigg) + (2\beta'\zeta\Omega-\alpha')\Bigg(1-\gamma' - \sum_{i=0}^{m-1}\gamma_i\Bigg)\Omega^2 - (1+\beta'\Omega^2)\Bigg(1-\gamma' \\ & - \sum_{i=0}^{m-1}\gamma_i\Bigg)\Omega^2 - \gamma'\Bigg(1-\Bigg(\frac{1}{2}-\beta' - \sum_{i=0}^{m-1}\beta_i\Bigg)\Omega^2\Bigg)\Omega^2(1+2\gamma'\zeta\Omega)\Bigg((1-\alpha' - \sum_{i=0}^{m-1}\alpha_i) - 2\Bigg(\frac{1}{2}-\beta' - \sum_{i=0}^{m-1}\beta_i\Bigg)\zeta\zeta\Bigg) \\ & -(2\beta'\zeta\Omega-\alpha')\Bigg(1-2(1-\gamma' - \sum_{i=0}^{m-1}\gamma_i)\zeta\zeta\Bigg) \\ & (1+\beta'\Omega^2)\Bigg(1-2(1-\gamma' - \sum_{i=0}^{m-1}\gamma_i)\zeta\zeta\Bigg) \\ & -\gamma'\Bigg((1-\alpha' - \sum_{i=0}^{m-1}\alpha_i) - 2\Bigg(\frac{1}{2}-\beta' - \sum_{i=0}^{m-1}\beta_i\Bigg)\zeta\zeta\Bigg)\Omega^2\Bigg]_{2\times2},\end{aligned} \tag{32}$$

$$\begin{aligned}\mathbf{A}^j_{2\times2} =& h_1\Big[-(1+2\gamma'\zeta\Omega)\beta_i\Omega^2 + (2\beta'\zeta\Omega-\alpha')\gamma_i\Omega^2 \\ & -(1+\beta'\Omega^2)\gamma_i\Omega^2 - \gamma'\beta_i\Omega^4(1+2\gamma'\zeta\Omega)(\alpha_i \\ & -2\beta_i\zeta\Omega) + 2\gamma_i\zeta\Omega(2\beta'\zeta\Omega-\alpha') - 2\gamma_i\zeta\Omega(1 \\ & +\beta'\Omega^2) - \gamma'(\alpha_i - 2\beta_i\zeta\Omega)\Omega^2\Big]_{2\times2}\end{aligned}$$

$$j = 1, 2, ..., m-1,$$

where Ω is natural frequency, i.e. $\Omega = \omega\Delta t$. In addition, parameter h_1 is defined as follows:

$$h_1 = \frac{1}{1+2\gamma'\zeta\Omega + (\beta'+\alpha'\gamma')\Omega^2}. \tag{33}$$

It should be noted that for studying the stability of G-IHOA integration, the weighted factors, i.e. α, β, and γ in the above matrices are used from Tables 1, 2, and 3. Moreover, the N-IHOA has only one set of independent weighted factors, and they are utilized from Table 3 [29]. Running similar procedure for IHOA leads to the following amplification matrices:

$$\begin{aligned}\mathbf{A}^0_{2\times2} =& h_2\Bigg[(1+2\eta_0\zeta\Omega)\Bigg(1-(\frac{1}{2}-\sum_{i=0}^{m-1}\zeta_i)\Omega^2\Bigg) \\ & + 2\zeta_0\zeta\Bigg(1-\sum_{i=0}^{m-1}\eta_i\Bigg)\Omega^3 - \eta_0\Omega^2\Bigg(1 \\ & -(\frac{1}{2}-\sum_{i=0}^{m-1}\zeta_i)\Omega^2\Bigg) - (1+\zeta_0\Omega^2)\end{aligned}$$

$$(1-\sum_{i=0}^{m-1}\eta_j)\Omega^2(1+2\eta_0\zeta\Omega)$$

$$\left(1-2(\frac{1}{2}-\sum_{i=0}^{m-1}\zeta_i)\zeta\Omega\right)$$

$$-2\zeta_0\zeta\Omega\left(1-2(1-\sum_{i=0}^{m-1}\eta_i)\zeta\Omega\right)(1+\zeta_0\Omega^2)$$

$$\left(1-2(1-\sum_{i=0}^{m-1}\eta_i)\zeta\Omega\right)-\eta_0\Omega^2\left(1\right.$$

$$\left.\left.-2(\frac{1}{2}-\sum_{i=0}^{m-1}\zeta_i)\zeta\Omega\right)\right]_{2\times 2}, \tag{34}$$

$$\mathbf{A}^j_{2\times 2}=h_2\begin{bmatrix}-(1+2\eta_0\zeta\Omega)\xi_j\Omega^2+2\xi_0\eta_j\zeta\Omega^3 & -2(1+2\eta_0\zeta\Omega)\xi_j\xi\Omega+4\xi_0\eta_j\zeta^2\Omega^2\\ \eta_0\xi_j\Omega^4-(1+\xi_0\Omega^2)\eta_j\Omega^2 & 2\eta_0\xi_j\zeta\Omega^3-2(1+\xi_0\Omega^2)\eta_j\zeta\Omega\end{bmatrix}_{2\times 2}$$

$$j=1,2,...,m-1$$

where parameter h_2 is defined as follows:

$$h_2=\frac{1}{1+2\eta_0\zeta\Omega+\xi_0\Omega^2}. \tag{35}$$

In these relationships, ξ and η are weighted factors of IHOA, and these values are employed from the reference paper [16].

Finally, Figures 1 to 4 show the maximum spectral radii of G-IHOA, N-IHOA, and IHOA integrations for different accuracy orders and various damping ratios which are calculated from the corresponding amplification matrices. From Figure 1, it is concluded that in undamped vibrations, all accuracy orders of N-IHOA and IHOA are unstable except $m = 1$. In this case, the first order of N-IHOA is unconditionally stable; however, the first order of IHOA is stable only for $\Omega \leq 3.464$. On the other hand, all orders of G-IHOA are conditionally stable so that they can provide wide range of stability for undamped vibrations. As a result, the proposed G-IHOA creates suitable stability bounds for dynamic analysis of common structures, which have low damping ($\zeta \to 0.0$, i.e. under-damped systems). Moreover, stability conditions of accuracy orders 2, 3, 4 and 5 of the proposed G-IHOA integration are approximately the same for $\zeta < 0.2$ (under-damped structures). This subject helps to utilize higher orders of the proposed integration which have higher accuracy without any concern about the numerical instability.

By increasing damping ratio, the stability bounds of G-IHOA decrease; however, the stability domain of

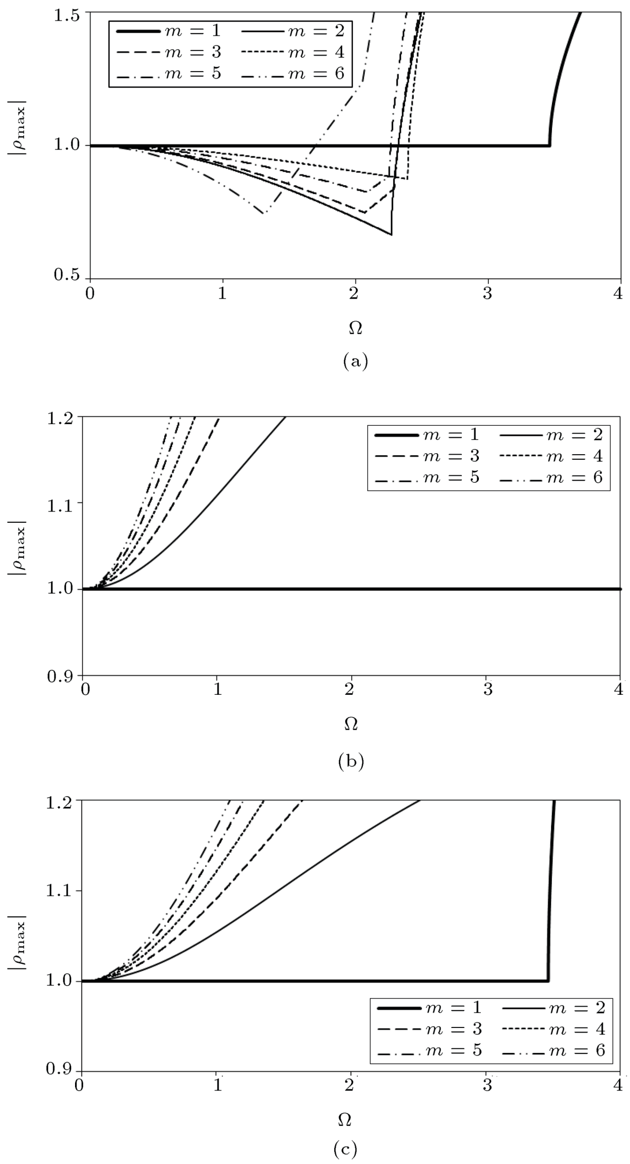

Figure 1. The maximum spectral radii of (a) G-IHOA, (b) N-IHOA, and (c) IHOA methods for $\zeta = 0.0$.

N-IHOA increases so that the most suitable stability condition for a system with critical damping ($\zeta = 1.0$) is provided by N-IHOA integration (Figure 3). As a result, G-IHOA and N-IHOA methods will be the most stable and efficient approaches for low and high damping models, respectively.

For better clarification of the above conclusions, the critical time steps of G-IHOA, N-IHOA, and IHOA methods are inserted in Table 4 for different damping ratios. It is clear that the proposed G-IHOA method always provides suitable domain for stability; however, IHOA and N-IHOA are unstable for some conditions.

Like the IHOA method, in G-IHOA and N-IHOA formulation, the time step is assumed constant. If time step is variable, weighted factors should be recomputed which is a complicated and time-consuming procedure.

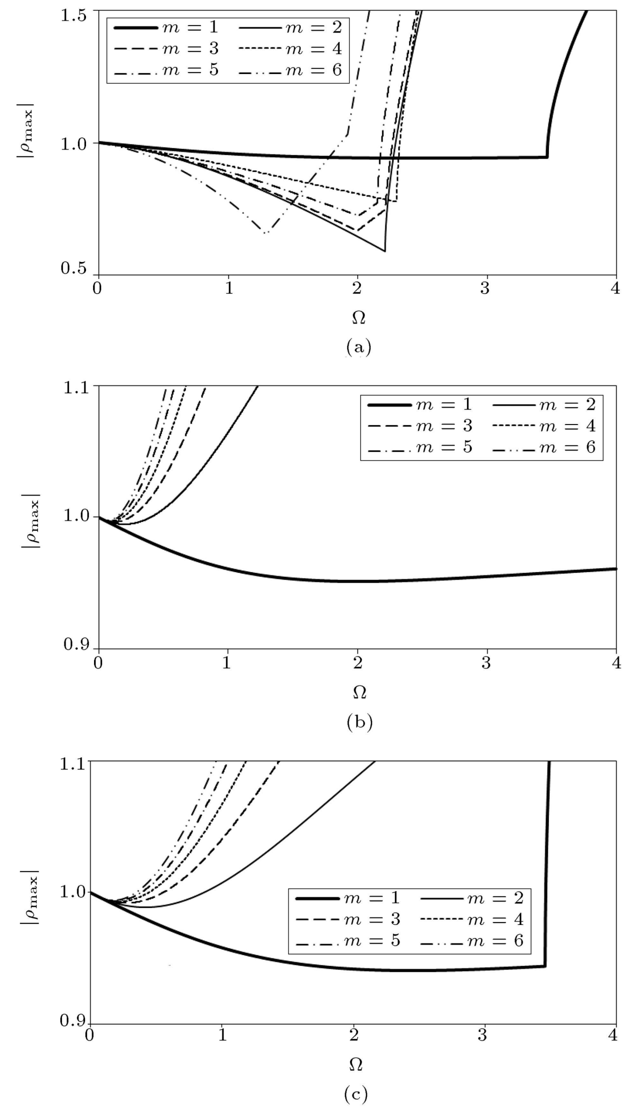

Figure 2. The maximum spectral radii of (a) G-IHOA, (b) N-IHOA, and (c) IHOA methods for $\zeta = 0.05$.

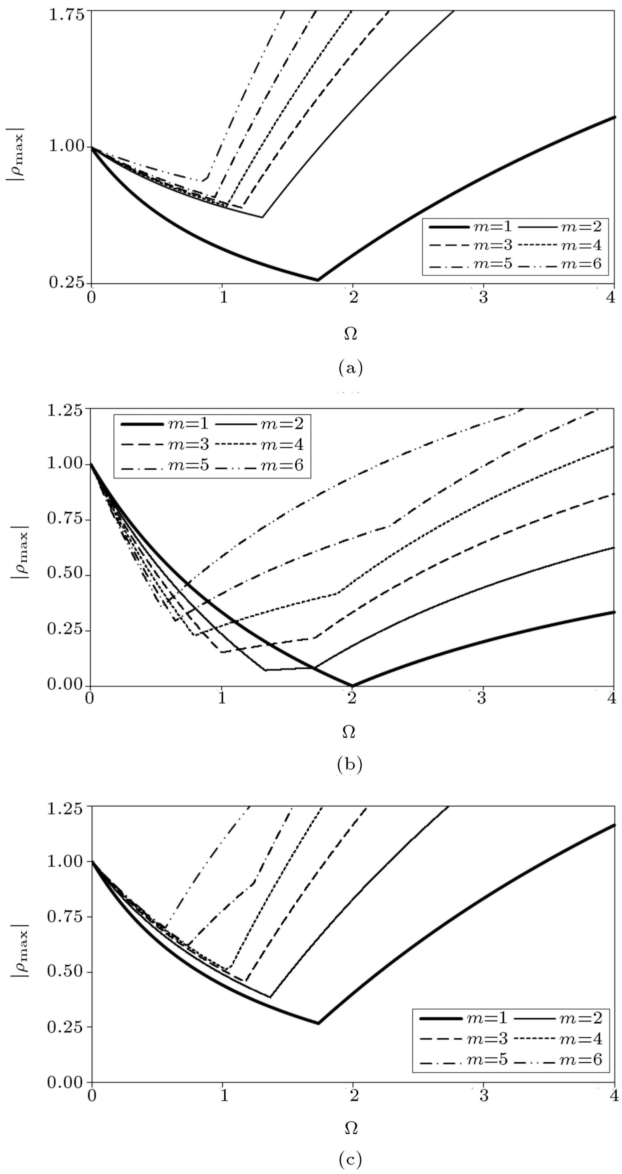

Figure 3. The maximum spectral radii of (a) G-IHOA, (b) N-IHOA, and (c) IHOA methods for $\zeta = 1.0$.

Using weighted factors of Tables 1 to 3 in the case of variable time steps causes some instability which may have minor effect on the overall response.

5. Numerical examples and discussion

In the previous sections, it was proved mathematically that the proposed G-IHOA integration is more accurate and stable compared with both N-IHOA and IHOA methods. Now, these conclusions should be verified numerically. Here, G-IHOA algorithm is utilized for analyzing some dynamic systems. For this purpose, a computer program using Fortran Power Station software (version 4) has been written by the author. Some benchmark problems, with available exact solutions, are solved to verify the validity of computer's program and numerical method. Then, a wide range of dynamic systems, such as linear and nonlinear, single and multi degree of freedom, damped and un-damped, free, and forced from finite element and finite difference, are used to compare the proposed integrations with other existing methods. For this purpose, results of G-IHOA (GI) are compared with those of some well-known methods such as the Newmark Linear Acceleration approach (LA), the Wilson-θ (WT), the trapezoidal method (CA), the N-IHOA scheme (NI), and the IHOA technique (IH).

It should be noted that in nonlinear dynamic analyses, system of Eq. (3) will be nonlinear. Here, *kinetic Dynamic Relaxation* (DR) method is employed to solve nonlinear system of Eq. (3) in each time step [34]. Simplicity, vector operators, and higher efficiency in nonlinear systems are other advantages of DR method [34,35]. As described in the recent

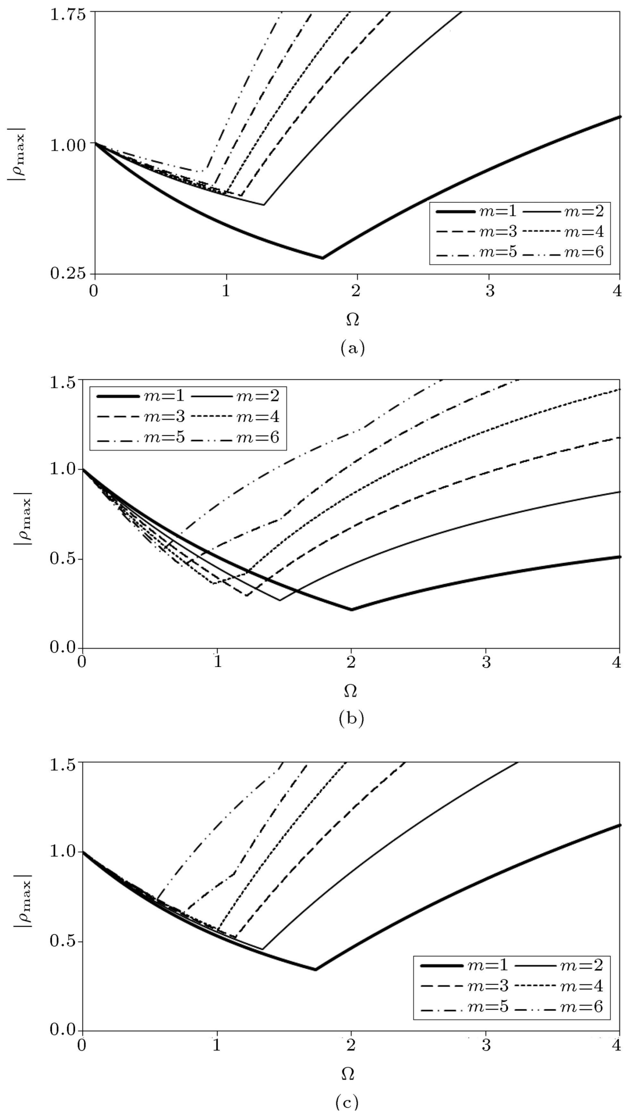

Figure 4. The maximum spectral radii of (a) G-IHOA, (b) N-IHOA, and (c) IHOA methods for $\zeta = 1.1$.

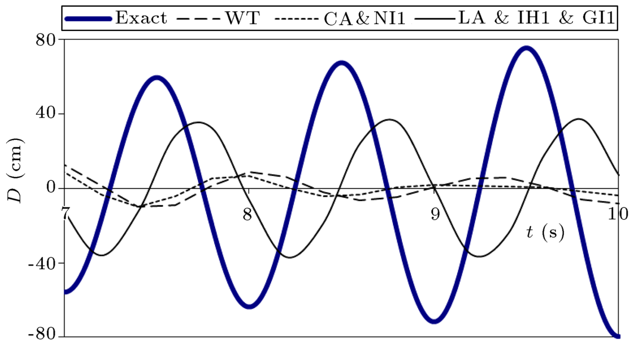

Figure 5. The response of the undamped SDOF system with the first order integrations.

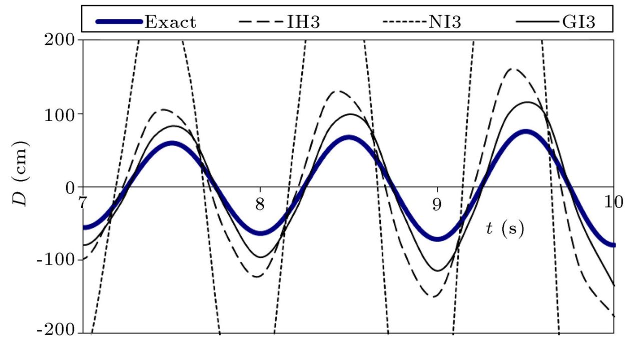

Figure 6. The response of the undamped SDOF system with the third order integrations.

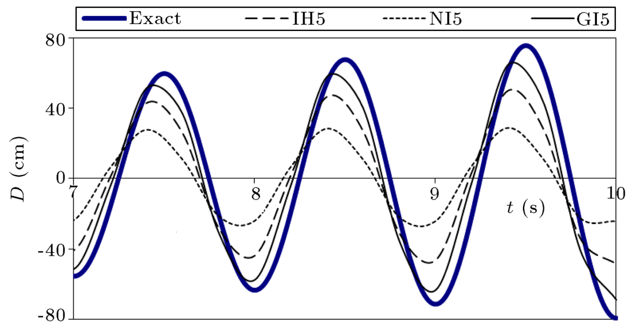

Figure 7. The response of the undamped SDOF system with the fifth order integrations.

papers, this method has been successfully combined with implicit time integrations so that it can cause a considerable reduction in numerical errors [34,36].

5.1. The linear single degree of freedom system

The first example deals with vibrations of a single degree of freedom system excited by a harmonic load [33]:

$$\ddot{d} + 2\pi\dot{d} + 4\pi^2 d = 100\sin(2\pi\pi),$$

$$d_{(0)} = 0.0 \qquad \dot{d}_{(0)} = 0.0. \tag{36}$$

The exact solution is calculated by elementary structural dynamics theories [33]. This system is analyzed in two cases, i.e. undamped ($\zeta = 0.0$) and damped ($\zeta = 0.2$) conditions. Because the natural period of this vibration is 1.0 s, the analysis is performed by time step of 0.2 s. Figures 5 to 7 show the numerical responses of undamped analysis achieved by various accuracy orders. In addition, the results of damped system are plotted in Figures 8 and 9. These figures clearly demonstrate that by the same integration's order, accuracy of the proposed G-IHOA integration is higher than those of both N-IHOA and IHOA methods. This higher accuracy could be seen in both damped and undamped conditions. Therefore, G-IHOA has suitable efficiency in both damped and undamped dynamic systems.

5.2. The elasto-plastic oscillator

The governing equation of a nonlinear vibration with elasto-plastic behavior is considered as follows [37]:

Table 4. The critical time steps for IHOA, N-IHOA, and G-IHOA integrations.

Damping ratio (ζ)	Integration method	Critical time step					
		$m=1$	$m=2$	$m=3$	$m=4$	$m=5$	$m=6$
0.00	IHOA	3.464	0.000	0.000	0.000	0.000	0.000
	N-IHOA	∞	0.000	0.000	0.000	0.000	0.000
	G-IHOA	3.464	2.322	2.323	2.402	2.268	1.699
0.05	IHOA	3.464	0.866	0.552	0.442	0.385	0.349
	N-IHOA	∞	0.399	0.239	0.182	0.151	0.131
	G-IHOA	3.464	2.288	2.267	2.324	2.183	1.863
0.10	IHOA	3.464	1.733	1.105	0.885	0.771	0.699
	N-IHOA	∞	0.799	0.479	0.364	0.302	0.262
	G-IHOA	3.464	2.255	2.213	2.249	2.103	1.836
0.20	IHOA	3.464	3.177	2.210	1.771	1.542	1.399
	N-IHOA	∞	1.599	0.959	0.729	0.605	0.525
	G-IHOA	3.464	2.191	2.109	2.106	1.952	1.704
1.00	IHOA	3.464	2.274	1.784	1.504	1.319	0.879
	N-IHOA	∞	∞	∞	3.645	3.025	2.209
	G-IHOA	3.464	1.744	1.456	1.293	1.134	0.987
1.10	IHOA	3.464	2.186	1.682	1.404	1.223	0.824
	N-IHOA	∞	∞	3.080	2.339	1.941	1.417
	G-IHOA	3.464	1.696	1.395	1.225	1.069	0.930

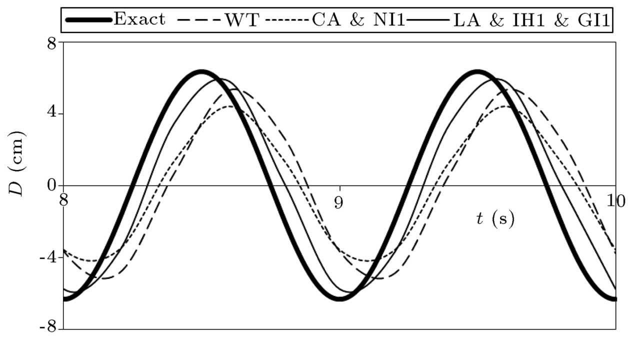

Figure 8. The response of the damped SDOF system with the first order integrations.

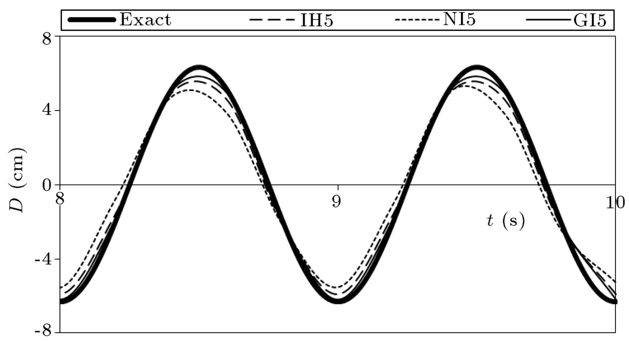

Figure 9. The response of the damped SDOF system with the fifth order integrations.

$$\ddot{d} + f_{(d)} = 0,$$

$$d_{(0)} = 0.0 \qquad \dot{d}_{(0)} = 25. \tag{37}$$

Here, the internal force, i.e. $f_{(d)}$, is an elastic-plastic function of displacement:

$$f_{(d)} = \begin{cases} 100d & |d| \leq 2.0 \\ 200 & d > 2.0 \\ -200 & d < -2.0 \end{cases} \tag{38}$$

Since the period of the vibration is 0.6729 s, the numerical analyses are run with time step as 0.06729 s. Figure 10, which shows the response of this nonlinear dynamic system, clearly demonstrates that GI method is more accurate than common approaches. In addition, by increasing the order of GI integration, the result's accuracy increases. On the other hand, Figures 11 and 12, which compare G-IHOA method with IHOA and N-IHOA integrations, show that by the same integration's order, G-IHOA method has more accuracy than both N-IHOA and IHOA techniques.

5.3. Two-bar pendulum

Figure 13 shows the pendulum formed by two bars hinged at each three ends. This system could be modeled by two truss elements, which have large

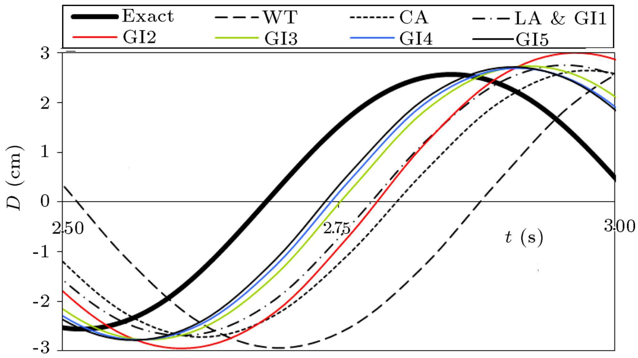

Figure 10. The response of the elasto-plastic system with time step of 0.06729 s.

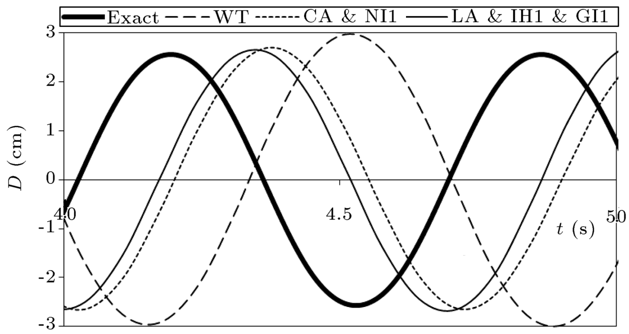

Figure 11. The response of the elasto-plastic system with the first order integrations.

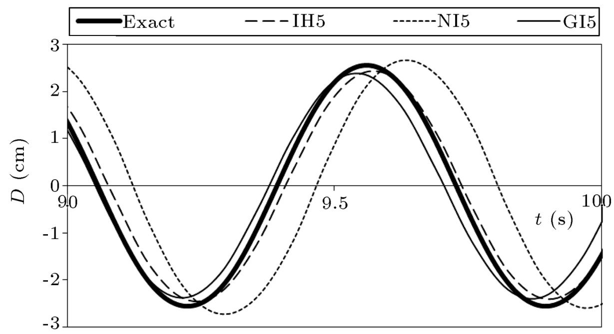

Figure 12. The response of the elasto-plastic system with the fifth order integrations.

deflection nonlinearity, modeled by the total Lagrange finite-element method [38]. Moreover, the mass matrix is consistent, [39] and the axial rigidity (AE) and material density per element length (ρA) are 10^4 N and 6.57 kg/m, respectively. An initial velocity as 7.72 m/s at its free end excites this system. For numerical analysis, a time step of 0.05 s is used. This high time step causes numerical instability in all of integrations except LA, IH1, GI1, GI2, and GI5. Figure 14 shows the vertical vibrations of the free end of the pendulum using time step 0.05 s, obtained by the stable methods (LA, IH1, GI1, GI2, and GI5). This example shows that G-IHOA integration provides more stable and accurate conditions for nonlinear structural dynamics

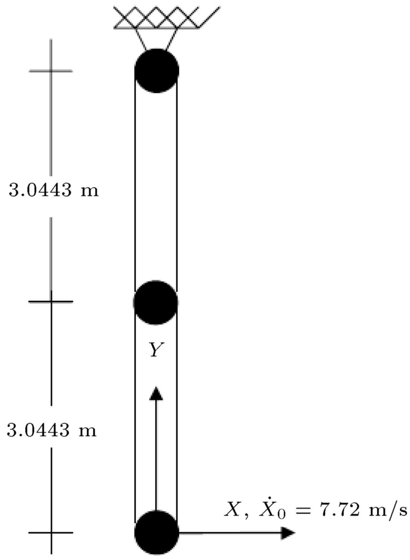

Figure 13. The two-bar elastic pendulum.

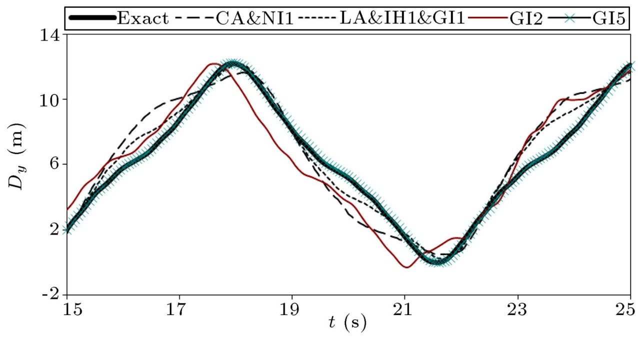

Figure 14. The vertical vibration of the free end of the pendulum with time step of 0.05 s.

in comparison with IHOA and N-IHOA. Another important point is the unique efficiency of GI5 method, which presents the exact solution by a high time step of 0.05 s. If this system is analyzed using a time step of 0.1 s, numerical errors grow dramatically, such that no integration methods could not come close to the answer, i.e. instability occurs in all numerical schemes. It should be noted that by reducing time step to 0.025 s, the proposed method with orders 1-5 (GI1, 2...5) would be stable; however, the integrations, such as IH2, NI2, and NI3, are still unstable.

5.4. Truss floor

Figure 15 shows a section of a floor covered by 2-D steel truss. Dynamic analysis of this truss under the impact, which is caused by the failure of the above floor, is the main goal of this example. For this purpose, the external forces, statically applied to the top node of truss, model the dead loads of the floor such as concrete slab and ceilings. Using these loads and running a static analysis, the deformed truss configuration is obtained (initial conditions for dynamic analysis). Now, the truss is subjected to an impact

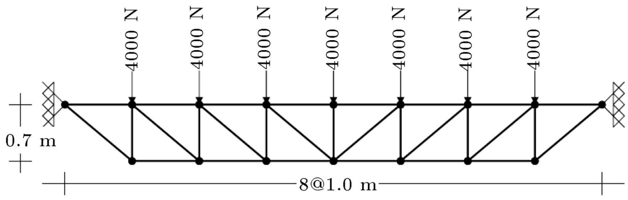

Figure 15. The truss floor.

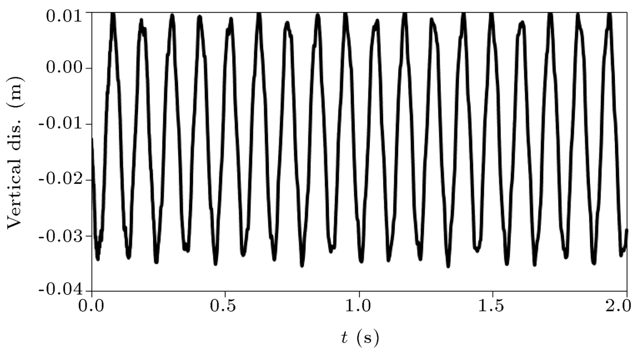

Figure 16. The vertical exact vibration of the upper central node of the truss floor.

that simulates the crashing of the above floor, i.e. the initial velocities of the upper seat nodes are assumed 10 m/s. Therefore, the analytical model is the undamped free vibration of the deformed truss under the initial velocities, which are calculated by the numerical time integrations. In these analyses, consistent mass matrix is constructed based on the truss element mass matrix [39]. Moreover, nonlinear elastic large deflection assumptions are used to construct the truss stiffness matrix [38]. For considering the effect of additional masses (floors, slabs, ceiling, etc.), the mass density of each element is assumed two times the density of steel, i.e. 15600 kg/m^3. Moreover, the modulus of elasticity of steel is $2.0e10$ N/m^2, respectively. The exact vertical vibration of the central upper node is plotted in Figure 16, using small time step, i.e. $1.0e-6$ s, in a higher order time integration [10]. Since the lowest truss period is 0.00236 s, time step of dynamic analysis is selected 0.00075 s. Using this time step causes numerical instability for all integrations except CA, LA, IH1, NI1, GI1, and GI5. Figure 17 shows vertical response of the upper central node, obtained from stable methods between times 1.9 s and 2.0 s. Like the previous example, the proposed GI5 is more accurate than other methods.

5.5. The frame building under the base excitation

The concrete building frame of Figure 18 [40] is excited by the El Centro base acceleration. This structure has elastic large deflection nonlinearity, which is modeled by the co-rotational finite-element method [38]. The cross-section and the moment of area of beams and

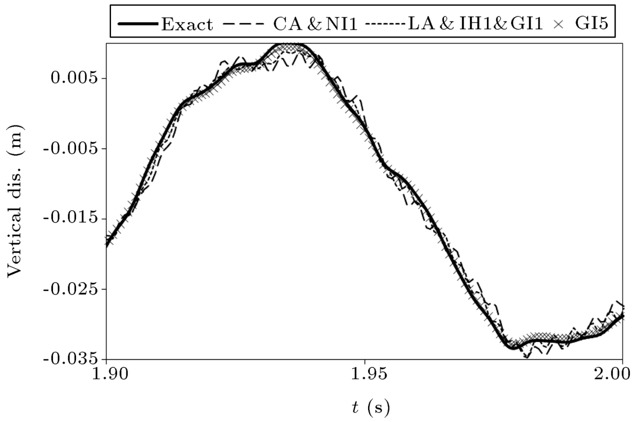

Figure 17. The vertical vibration of the upper central node of the truss floor with time step of 0.00075 s between 1.9-2.0 s.

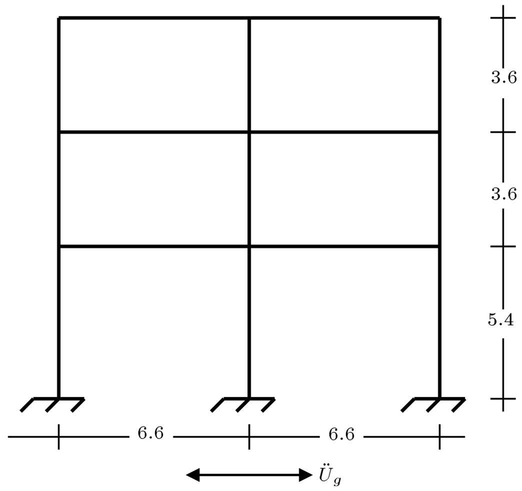

Figure 18. The portal frame under the base excitation.

columns are 0.40 m^2, 0.03333 m^4, 0.64 m^2, and 0.03413 m^4, respectively. In order to construct the consistent mass matrix of each beam and column of frame [39], the mass density of concrete is assumed 2500 kg/m^3. This structure is analyzed when the damping factor of the first, second, and third vibration modes are 10%, 5%, and 3%, respectively [33]. Figure 19 shows the quasi-exact response of the horizontal displacement of the top of the frame. As the lowest time period is 0.003313 s, the time step of numerical analysis is selected as 0.001 s. Using this time step causes CA, LA, IH1, NI1, GI1, and GI5 integrations to present the quasi-exact vibration (Figure 19). Therefore, the fifth order of the proposed integration (GI5) is more accurate than IH5 and NI5 methods. Consequently, in the same order and time step, G-IHOA is more accurate than IHOA and N-IHOA. It should be noted that by reducing time step to 0.0008 s, some other methods, such as IH4, IH5, and GI4, also present the exact solution.

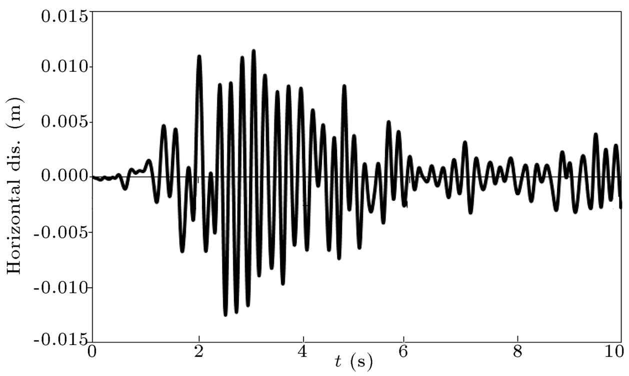

Figure 19. The horizontal exact vibration of the top of the portal frame.

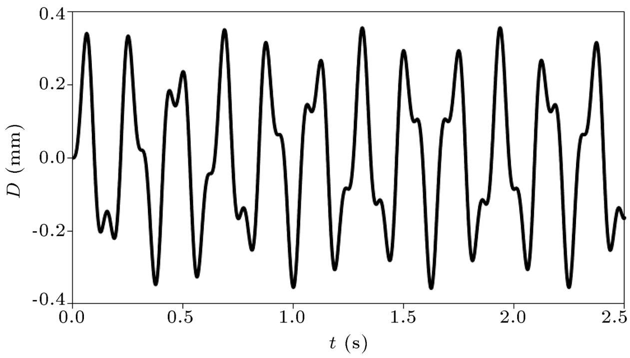

Figure 20. The exact vibration of the central displacement of Euler beam.

5.6. Euler beam

Here, Euler beam's theory is utilized for dynamic analysis of a simply supported beam, which has the following governing equation of motion [4]:

$$\rho A\frac{\partial^2 d}{\partial t^2}+\frac{\partial^2}{\partial x^2}\left(E1\frac{\partial^2 d}{\partial x^2}\right)=p_{(x,t)}. \tag{39}$$

The boundary conditions of simply supported Euler beam give:

$$d_{(0,t)}=0, \quad EI\frac{\partial^2 D}{\partial x^2}|_{x=0}=0,$$

$$d_{(L,t)}=0, \quad EI\frac{\partial^2 D}{\partial x^2}|_{x=L}=0. \tag{40}$$

This structure is analyzed under the external harmonic load applied to the mid-span of the beam with zero initial conditions as follows:

$$p_{(0.5L,t)}=88.968\sin(30.0t)\text{N}. \tag{41}$$

The length of beam, the material density, the modulus of elasticity, the cross-section, and the moment of area are 0.508 m, 2768 kg/m^3, 6.897×10^{10} N/m^2, 6.4516×10^{-4} m^2, and 3.4686×10^{-8} m^4, respectively. There are different methods for modelling and formulating the dynamic equilibrium equations. The Finite-difference technique is one of these methods which could directly use for dynamic modelling of systems. Studying the efficiency of time integrations in problems modeled by finite-difference approach is the main goal of this section. Therefore, the finite-differences approach is utilized to obtain the dynamic equilibrium equations of the Euler beam. By using one-dimensional mesh and central finite differences method, the dynamic equilibrium equation for the ith node of mesh is as follows:

$$\rho A\frac{\partial^2 d_i}{\partial t^2}+EI\frac{d_{i+2}-4d_{i+1}+6d_i-4d_{i-1}+d_{i-2}}{(\Delta x)^4}$$
$$=p_{(x_i,t)}. \tag{42}$$

Here, Δx is the distance between mesh nodes, assumed constant. Here, a mesh with eleven nodes (Δx = 0.0508 m) is considered. All boundary conditions are also expressed by the central finite differences method. As a result, a linear system of dynamic equations is obtained. At this stage, numerical time integrations are used to calculate the time response of beam. Figure 20 shows the quasi-exact vibration of the central displacement of beam, achieved by very small time step, i.e. 5e-6 s. The minimum period of the beam is 0.00223 s. In this example, the highest time step for obtaining the exact vibration of the beam is determined. Results, inserted in Table 5, show that for the same integration's order, the proposed G-IHOA method is more accurate than IHOA and N-IHOA. For example, the maximum time steps of GI5, IH5, and NI5 for converging to the quasi-exact vibration are 0.0007, 0.0005, and 0.00045 s, respectively. In other words, G-IHOA could present the exact vibrations by larger time step that reduces the computational time. This subject could also be clearly recognized for other accuracy orders (Table 5). Moreover, this example shows that the proposed time integration could be successfully used for dynamic analysis of systems modeled by finite differences method.

6. Conclusion

The generalized implicit multi-time-step integration

Table 5. The highest possible time step for obtaining the exact vibration of the Euler beam.

Integration method	CA, LA, IH1, GI1	NI1, GI5	IH5	NI5	IH4, NI4, GI4	GI3	IH3	NI3, GI2	IH2, NI2
$\Delta t_{\max}$ (s)	0.00075	0.00070	0.00050	0.00045	0.00040	0.00025	0.00020	0.00015	0.00010

was proposed here for the numerical dynamic analysis. This formulation led to two new kinds of integrations called the G-IHOA and the N-IHOA. Based on using the accelerations and velocities of some previous steps, the G-IHOA has three groups of integration's parameters and the N-IHOA has only one set of independent weighted factors. The numerical values of these parameters were calculated from the minimization of the displacement and velocity's residuals in the Taylor series. This procedure proved that the displacement accuracy order of the proposed G-IHOA (Δt^{2m+2}) is higher than those of IHOA (Δt^{m+3}) and N-IHOA (Δt^{m+2}). In addition, the mathematical stability analysis, performed based on the amplification matrices, demonstrated that the G-IHOA method always provides suitable stability domain so that it is not unstable in any condition. For undamped vibrations, the higher orders of both IHOA and N-IHOA ($m > 1$) will be unstable; however, the higher orders of the G-IHOA integration are stable. Moreover, the stability analysis clarified that another proposed integration (N-IHOA) is more suitable for high damping system. On the other hand, a wide range of numerical studies (single/multi degrees of freedom, damped/un-damped, free/forced vibrations from finite element/finite difference) demonstrate that by the same accuracy order and time step, the accuracy of the proposed G-IHOA method is higher than those of other existing techniques like the IHOA integration. This subject can be clearly concluded from all examples. Therefore, the efficiency and accuracy of the G-IHOA do not depend on the structural specifications such as number of degrees of freedom, type of loading, structural behavior (linear/nonlinear, damped/undamped), etc. Unique numerical accuracy and suitable efficiency and stability of the fifth order of the proposed G-IHOA method, i.e. GI5, is another important point, outlined by these examples.

References

1. Hilber, H.M., Hughes, T.J.R. and Taylor, R.L. "Improver numerical dissipation for time integration algorithm in structural dynamics", *Earthquake Engineering & Structural Dynamics*, **5**(3), pp. 283-292 (1977).
2. Wood, W.L., Bossak, M. and Zienkiewicz, O.C. "An alpha modification of Newmark's method", *International Journal for Numerical Methods in Engineering*, **15**(10), pp. 1562-1566 (1981).
3. Chung, J. and Hulbert, G.M. "A time integration method for structural dynamics with improved numerical dissipation: the generalized α-method", *Journal of Applied Mechanics*, **60**(2), pp. 371-384 (1993).
4. Kim, S.J., Cho, J.Y. and Kim, W.D. "From the trapezoidal rule to higher order accurate and unconditionally stable time-integration method for structural dynamics", *Computer Methods in Applied Mechanics and Engineering*, **149**(1-4), pp. 73-88 (1997).
5. Fung, T.C. "Third order time-step integration methods with controllable numerical dissipation", *Communications in Numerical Methods in Engineering*, **13**(4), pp. 307-315 (1997).
6. Fung, T.C. "Complex-time-step Newmark methods with controllable numerical dissipation", *International Journal for Numerical Methods in Engineering*, **41**(1), pp. 65-93 (1998).
7. Tamma, K.K., Zhou, X. and Sha, D. "A theory of development and design of generalized integration operators for computational structural dynamics", *International Journal for Numerical Methods in Engineering*, **50**(7), pp. 1619-1664 (2001).
8. Modak, S. and Sotelino, E.D. "The generalized method for structural dynamic applications", *Advances in Engineering Software*, **33**(7-10), pp. 565-575 (2002).
9. Mancuso, M. and Ubertini, F. "The Norsett time integration methodology for finite element transient analysis", *Computer Methods in Applied Mechanics and Engineering*, **191**(29-30), pp. 3297-3327 (2002).
10. Bathe, K.J. and Baig, M.M.I. "On a composite implicit time integration procedure for nonlinear dynamics", *Computers and Structures*, **83**(31-32), pp. 2513-2524 (2005).
11. Keierleber, C.W. and Rosson, B.T. "Higher-order implicit dynamic time integration method", *Journal of Structural Engineering ASCE*, **131**(8), pp. 1267-1276 (2005).
12. Bathe, K.J. "Conserving energy and momentum in nonlinear dynamics: A simple implicit time integration scheme", *Computers and Structures*, **85**(7-8), pp. 437-445 (2007).
13. Soares, D. and Mansur, W.J. "A frequency-domain FEM approach based on implicit Green's functions for non-linear dynamic analysis", *International Journal of Solids and Structures*, **42**(23), pp. 6003-6014 (2005).
14. Loureiro, F.S. and Mansur, W.J. "A novel time-marching scheme using numerical Green's functions: A comparative study for the scalar wave equation", *Computer Methods in Applied Mechanics and Engineering*, **199**(23-24), pp. 1502-1512 (2010).
15. Wang, M.F. and Au, F.T.K. "Precise integration methods based on Lagrange piecewise interpolation polynomials", *International Journal for Numerical Methods in Engineering*, **77**(7), pp. 998-1014 (2009).
16. Rezaiee-Pajand, M. and Alamatian, J. "Implicit higher order accuracy method for numerical integration in dynamic analysis", *Journal of Structural Engineering ASCE*, **134**(6), pp. 973-985 (2008).
17. Regueiro, R.A. and Ebrahimi, D. "Implicit dynamic three-dimensional finite element analysis of an inelastic biphasic mixture at finite strain", *Computer Methods in Applied Mechanics and Engineering*, **199**(29-32), pp. 2024-2049 (2010).
18. Zienkiewicz, O.C., Wood, W.L., Hine, N.W. and Taylor, R.L. "A unified set of single step algorithms. Part

1: General formulation and applications", *International Journal for Numerical Methods in Engineering*, **20**(8), pp. 1529-1552 (1984).

19. Wood, W.L. "A unified set of single step algorithms. Part 2: Theory", *International Journal for Numerical Methods in Engineering*, **20**(12), pp. 2303-2309 (1984).

20. Katona, M.C. and Zienkiewicz, O.C. "A unified set of single step algorithms Part 3: The beta-m method, A generalization of the Newmark scheme", *International Journal for Numerical Methods in Engineering*, **21**(7), pp. 1345-1359 (1985).

21. Hoff, C. and Taylor, R.L. "Higher derivative explicit one step methods for non-linear dynamic problems. Part I: Design and theory", *International Journal for Numerical Methods in Engineering*, **29**(2), pp. 275-290 (1990).

22. Zhai, W.M. "Two simple fast integration methods for large-scale dynamic problems in engineering", *International Journal for Numerical Methods in Engineering*, **39**(24), pp. 4199-4214 (1996).

23. Zhang, Y., Sause, R., Ricles, J.M. and Naito, C.J. "Modified predictor-corrector numerical scheme for real-time pseudo dynamic tests using state-space formulation", *Earthquake Engineering & Structural Dynamics*, **34**(3), pp. 271-288 (2005).

24. Rezaiee-Pajand, M. and Alamatian, J. "Numerical time integration for dynamic analysis using new higher order predictor-corrector method", *Journal of Engineering Computations*, **25**(6), pp. 541-568 (2008).

25. Zuijlen, A.H.V. and Bijl, H. "Implicit and explicit higher order time integration schemes for structural dynamics and fluid-structure interaction computations", *Computers and Structures*, **83**(2-3), pp. 93-105 (2005).

26. Rama Mohan Rao, M. "A parallel mixed time integration algorithm for nonlinear dynamic analysis", *Advances in Engineering Software*, **33**(5), pp. 261-271 (2002).

27. Zhou, X. and Tamma, K.K. "Design, analysis, and synthesis of generalized single step single solve and optimal algorithms for structural dynamics", *International Journal for Numerical Methods in Engineering*, **59**(5), pp. 597-668 (2004).

28. Smolinski, P., Belytschko, T. and Neal, M. "Multi-time-step integration using nodal partitioning", *International Journal for Numerical Methods in Engineering*, **26**(2), pp. 349-359 (1988).

29. Alamatian, J. "New implicit higher order time integration for dynamic analysis", *Structural Engineering and Mechanics*, **48**(5), pp. 711-736 (2013).

30. Wiberg, N.E. and Li, X.D. "A post- processing technique and an α posteriori error estimate for the Newmark method in dynamic analysis", *Earthquake Engineering & Structural Dynamics*, **22**(6), pp. 465-489 (1993).

31. Gobat, J.I. and Grosenbaugh, M.A. "Application of the generalized-α method to the time integration of the cable dynamics equations", *Computer Methods in Applied Mechanics and Engineering*, **190**(37-38), pp. 4817-4829 (2001).

32. Pegon, P. "Alternative characterization of time integration schemes", *Computer Methods in Applied Mechanics and Engineering*, **190**(20-21), pp. 2707-2727 (2001).

33. Clough, R.W. and Penzien, J., *Dynamics of Structures*, McGraw Hill, New York (1993).

34. Alamatian, J. "A new formulation for fictitious mass of the Dynamic Relaxation method with kinetic damping", *Computers and Structures*, **90-91**, pp. 42-54 (2012).

35. Kadkhodayan, M., Alamatian, J. and Turvey, G.J. "A new fictitious time for the Dynamic Relaxation (DXDR) method", *International Journal for Numerical Methods in Engineering*, **74**(6), pp. 996-1018 (2008).

36. Rezaiee-Pajand, M. and Alamatian, J. "Nonlinear dynamic analysis by Dynamic Relaxation method", *Journal of Structural Engineering and Mechanics*, **28**(5), pp. 549-570 (2008).

37. Hoff, C. and Taylor, R.L. "Higher derivative explicit one step methods for non-linear dynamic problems. Part II: Practical calculations and comparison with other higher order methods", *International Journal for Numerical Methods in Engineering*, **29**(2), pp. 291-301 (1990).

38. Felippa, C.A., *Nonlinear Finite Element Methods*. <http:// www.colorado.edu /courses.d /nfemd/> (Feb. 10 2002) (1999).

39. Paz, M., *Structural Dynamics: Theory and Computation*, McGraw Hill, New York (1979).

40. Liu, Q., Zhang, J. and Yan, L. "A numerical method of calculating first and second derivatives of dynamic response based on Gauss precise time step integration method", *European Journal of Mechanics A/Solids*, **29**(3), pp. 370-377 (2010).

Appendix

Matrices $[Z_D]$ and $[Z_V]$ for the integration's orders 1, 2, and 3:

$$[Z_D]=\begin{bmatrix}1 & 0\\ 0.5 & 1\end{bmatrix} \qquad [Z_V]=[1] \qquad m=1, \tag{A.1}$$

$$[Z_D]=\begin{bmatrix}1 & -1 & 0 & 0\\ 0.5 & 0.5 & 1 & -1\\ 0.1667 & -0.1667 & 0.5 & 0.5\\ 0.0417 & 0.0417 & 0.1667 & -0.1667\end{bmatrix},$$

$$[Z_V]=\begin{bmatrix}1 & -1\\ 0.5 & 0.5\end{bmatrix} \qquad m=2, \tag{A.2}$$

$$[Z_D] = \begin{bmatrix} 1 & -1 & -2 & 0 & 0 & 0 \\ 0.5 & 0.5 & 2 & 1 & -1 & -2 \\ 0.1667 & -0.1667 & -1.3333 & 0.5 & 0.5 & 2 \\ 0.0417 & 0.0417 & 0.6667 & 0.1667 & -0.1667 & -1.3333 \\ 0.0083 & -0.0083 & -0.2667 & 0.0417 & 0.0417 & 0.6667 \\ 0.0014 & 0.0014 & 0.0889 & 0.0083 & -0.0083 & -0.2667 \end{bmatrix},$$

$$[Z_V] = \begin{bmatrix} 1 & -1 & -2 \\ 0.5 & 0.5 & 2 \\ 0.1667 & -0.1667 & -1.3333 \end{bmatrix} \quad m = 2. \tag{A.3}$$

Biography

Javad Alamatian is an Assistant Professor in Civil Engineering Department of Islamic Azad University of Mashhad, Mashhad, Iran. He received his PhD degree in Structural Engineering from Ferdowsi University of Mashhad. His research interests include numerical methods, dynamic analysis, time integration, nonlinear analysis, dynamic relaxation and structural control.